

Highly oriented planar arrays of SWCNTs grown onto HOPG substrates by means of an ‘all-laser’ process

J.H. Yi, M.A. El Khakani *

Institut National de la Recherche Scientifique, INRS-Énergie, Matériaux et Télécommunications, 1650 Boulevard Lionel-Boulet, C.P. 1020, Varennes, Que., Canada J3X 1S2

Received 31 March 2005; in final form 8 July 2005
Available online 15 August 2005

Abstract

We report on an ‘all-laser’ approach for the growth of highly oriented planar (2D) arrays of single wall carbon nanotubes (SWCNTs) onto HOPG substrates. This growth process uses the same KrF laser to deposit, in a first step, the CoNi nanoparticles onto HOPG and then to grow, in a subsequent step, the SWCNTs from the ablation of a pure graphite target. It is shown that the laser-grown 2D arrays of SWCNTs exhibit not only a very narrow diameter distribution (~ 1 nm-diam.) but more notably a strong alignment over the underlying HOPG lattice. The ‘all-laser’ process is also shown to be extremely efficient in converting the laser-ablated graphite into SWCNTs.

© 2005 Elsevier B.V. All rights reserved.

1. Introduction

Single-wall carbon nanotubes (SWCNTs) are among the most promising building blocks for future nanoelectronic devices because of their unpaired intrinsic properties [1–3]. In order to take the best advantage of their unique electrical properties for the achievement of practical nanodevices, it is highly desirable to be able to assemble them at will in any desired position and/or orientation [4,5]. The localized growth of SWCNTs on catalyst-patterned substrates has been shown to be a very attractive approach for guiding the self-assembly of SWCNTs and their subsequent integration into devices with a minimum of post-growth processing [6,7]. Chemical vapor deposition (CVD) is one of the most widely used techniques for the localized growth of SWCNTs between patterned catalyst islands which can also serve as direct electrical contacts [6–10]. It has been also used with the assistance of electric or magnetic fields to grow oriented SWCNTs onto patterned surfaces [7,9,10].

The laser vaporization is an alternative approach that has been shown to synthesize SWCNT with the highest purity (up to $\sim 90\%$) and a narrow diameter distribution [11,12]. While the first demonstration of laser synthesis of SWCNTs was achieved by means of a Nd:YAG laser [13], we have recently shown that SWCNTs can be also synthesized by means of a KrF ultraviolet (UV) laser [14], at a furnace temperature rather lower than that required when visible and/or infrared lasers are used. In the standard scheme of laser synthesis of SWCNTs, the nanotube growth is achieved through the laser ablation of a graphite target doped with metal catalyst in a controlled gas atmosphere [13–16]. Thus, the laser-ablated mixture of carbon and metal catalyst leads to the growth of SWCNTs until the system has sufficiently cooled that carbon no longer can diffuse through the catalyst particles [11,15]. In contrast, in the absence of any metal catalyst, the laser vaporization of a graphite target does not lead to an effective growth of carbon nanotubes; it yields rather other carbon nanostructures (such as fullerenes, nanohorns or graphitic nanocages), regardless of the used laser wavelength [17–19]. The integration of laser-grown SWCNTs into electronic devices

* Corresponding author.

E-mail address: elkhakani@emt.inrs.ca (M.A. El Khakani).

requires their subsequent purification, then sorting them out from the soot, followed by cutting and nano-manipulation for their precise positioning between patterned electrodes [4,20]. To avoid this laborious post-processing effort, we have very recently developed an ‘all-laser’ growth approach that permits the localized growth of SWCNTs and their direct integration into field-effect like devices [21]. This novel ‘all-laser’ process is distinguished by its exclusive use of the same pulsed KrF excimer laser, first, to deposit CoNi catalyst nanoparticles of controllable size at specific locations on pre-patterned substrates and, second, to grow SWCNTs onto those catalyst locations through the pulsed laser ablation of a pure graphite target.

In this Letter, we report on the use of the ‘all-laser’ approach to grow highly aligned SWCNTs onto HOPG substrates. The on-substrate laser-grown SWCNTs are shown, for the first time, not only to self-organize into planar (2D) arrays but also to present a specific tube axis orientation that is parallel to the underlying HOPG crystallographic planes. This sort of epitaxial growth of SWCNTs clearly opens up new possibilities for the controlled assembly of SWCNTs and for their application for nanodevices.

2. Experimental

Prior to the carbon nanotube growth, CoNi catalyst nanoparticles were first deposited on freshly cleaved HOPG substrates by pulsed laser deposition (PLD) using a KrF excimer laser ($\lambda = 248$ nm; pulse duration = 15 ns). As nanotube growth is known to be strongly influenced by the size of catalyst nanoparticles [22,23], we have identified the PLD conditions that lead to the growth of CoNi nanoparticles with diameters of ~ 1 nm. These conditions include an on-target laser intensity of $\sim 4 \times 10^8$ W/cm² and a background He pressure of 300 mTorr for a target–substrate distance of 5 cm. The CoNi nanoparticle-decorated HOPG substrates were then used to grow carbon nanotubes by laser-ablating a pure graphite target in a controlled Ar atmosphere (1–5 Torr pressure) at a furnace temperature of 1150 °C. The laser intensity on the graphite target was in the $(2\text{--}5) \times 10^8$ W/cm² range, which was found to be optimal for the growth of SWCNTs by means of a KrF laser [14,18]. It is important to note here that in our ‘all-laser’ process, the SWCNT growth occurs on the substrate through the interaction of the laser ablated carbon vapor with the pre-deposited CoNi nanoparticles. Thus, the amount of ablated graphite carbon can be controlled (independently of the catalyst nanoparticles), by varying the number of laser ablation pulses, to ensure an efficient interaction with the CoNi catalyst nanoparticles. As-deposited CoNi nanoparticles and the nanotubes grown on HOPG were characterized

by scanning tunneling microscopy (STM, NanoScope III, Digital Instrument (DI)) and micro-Raman spectroscopy (Renishaw Imaging Microscope Wire™, $\lambda = 514.5$ nm) in air at room temperature. The STM was operated in constant height mode with a bias voltage of 500 mV and a tunneling current of 1 nA. The STM scanner was calibrated in two subsequent steps: firstly by means of a calibration grid of 10 nm height (from DI) and then by a step-edge of HOPG.

3. Results and discussion

Fig. 1a shows a typical STM image of the CoNi nanoparticles deposited on HOPG substrates under the PLD

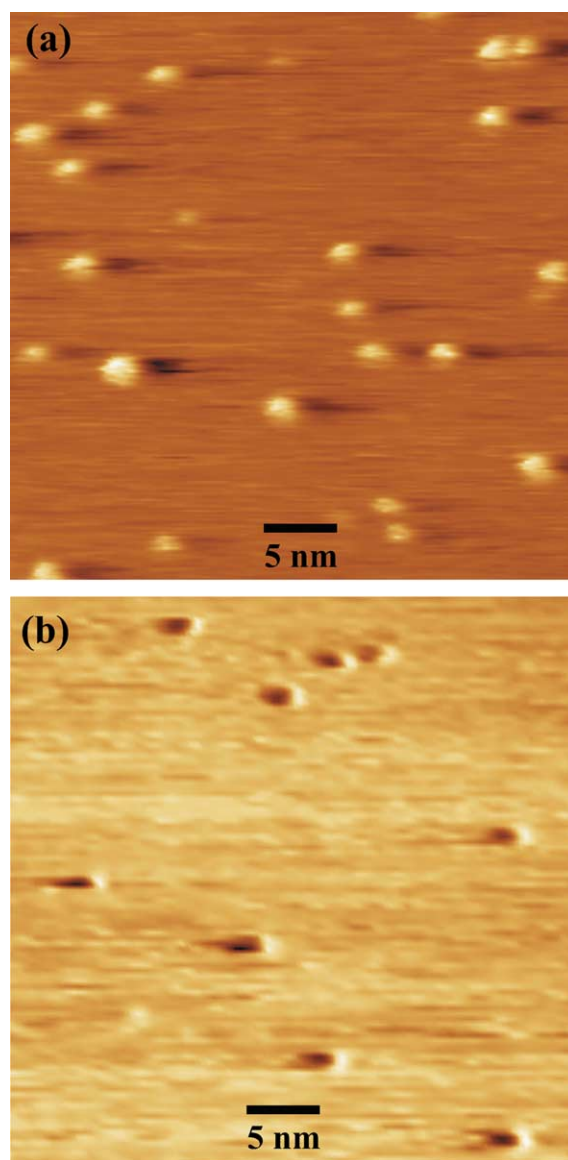


Fig. 1. Typical STM images of CoNi nanoparticles deposited on HOPG surface with 20 laser ablation pulses: (a) as-deposited, and (b) after a heat treatment at 1150 °C.

conditions just described. Fig. 1a clearly shows that discrete CoNi nanoparticles are well dispersed on the HOPG surface with an average diameter of 1.1 ± 0.2 nm and a surface density of $\sim 1.5 \times 10^{12} \text{ cm}^{-2}$. Since the carbon nanotube growth is carried out at high temperature, we have investigated possible morphological changes of the CoNi nanoparticles on HOPG substrates following a heat treatment that simulates the nanotube growth conditions (i.e., 10 min at 1150 °C in Ar atmosphere). As shown in Fig. 1b, the surface density of the nanoparticles is found to be reduced by a factor of ~ 2.7 (to a value of $\sim 5.6 \times 10^{11} \text{ cm}^{-2}$), while the mean diameter of the nanoparticles increased slightly to 1.2 ± 0.2 nm. (Such a nanoparticle diameter is favorable for the nucleation and growth of SWCNTs according to the theoretical work of [24].) These changes are thought to be the result of two competing effects: (i) the diffusion-favored coalescence of small particles to form larger ones, but counteracted by (ii) some material loss through evaporation (which is expected to occur at temperatures lower than those of the bulk because of the nanometer size of the particles [25]). As illustrated in Fig. 1b, STM observations did not reveal any nanotube formation on the HOPG substrate decorated with CoNi nanoparticles and simply heat-treated at 1150 °C. This was also confirmed by the Raman spectroscopy analyses (shown later in Fig. 3a) where only the HOPG characteristic peak is present with no carbon nanotube related peaks. These results clearly show that the carbon vapor source (provided through the ablation of the graphite target in the second step of the ‘all-laser’ process) is a prerequisite for the growth of SWCNTs on the HOPG substrates decorated with CoNi nanoparticles.

Fig. 2 shows STM images of HOPG surfaces (with and without CoNi nanoparticles) after their exposure to 100 laser ablation pulses of the graphite target at 1150 °C under argon. (Such an amount of ablated carbon would correspond to an equivalent coating layer of ~ 4 nm-thick.) In the absence of CoNi catalyst nanoparticles, Fig. 2a confirms that no carbon nanotubes were formed and only some elongated shingle-like carbon nanostructures are present on the HOPG substrates. In contrast, when the carbon deposition was carried out on CoNi nanoparticle-decorated HOPG substrates, the STM image (Fig. 2b) revealed the presence of highly aligned arrays of carbon nanotubes on the HOPG surface. The average tube diameter (1.10 ± 0.26 nm, measured from the heights of at least 50 tubes in STM images) confirms that the 1D structures are single wall carbon nanotubes. (This nanotube diameter will be unambiguously confirmed from Raman spectroscopy analyses hereafter.) The average tube length with the 100 laser ablation pulses was found to be of ~ 80 nm. Nevertheless, some nanotubes having up to 200 nm in length were also observed (not shown) to grow between two CoNi catalyst islands. Bumps gen-

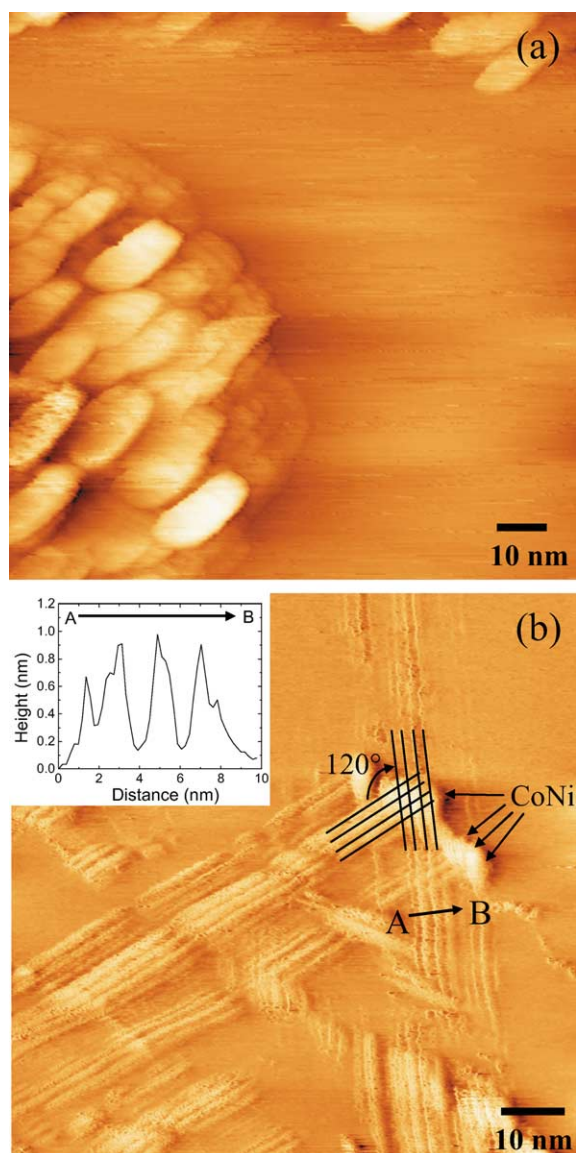


Fig. 2. Typical STM images of HOPG surfaces after deposition of 100 laser ablation pulses of carbon at 1150 °C (a) on bare HOPG surface, and (b) on HOPG surface decorated with CoNi catalyst nanoparticles. The inset is a linescan height profile along the A–B arrow in (b).

erally located at the junctions of two differently oriented SWCNT arrays (black arrows in Fig. 2b) are highly likely due to the CoNi catalyst nanoparticles. Their actual size and morphology are slightly different from those of CoNi nanoparticles subjected to the heat treatment (Fig. 1b), as they appear to be slightly elongated with a larger size (~ 2.5 nm). These observations may, however, result from their covering by the SWCNT arrays and/or additional coalescence during nanotube formation. It is worth noting here that transmission electron microscopy observations of SWCNTs grown by the same ‘all-laser’ process onto free-standing, very thin Si_3N_4 membranes confirmed that CoNi nanoparticles are usually located at the crossings of different SWCNT bundles. (Bundles in their early growth stages

can be seen to root from CoNi nanoparticles.) [26]. Beside the fact that the underlying substrate plays a determining role on the orientation and structural arrangements of the SWCNTs (as shown here for HOPG versus Si_3N_4 where randomly networked 3D-bundles are obtained), these results suggest that the ‘all-laser’ synthesized SWCNT bundles grow from CoNi nanoparticles.

Unlike the classical laser ablation scheme, where the SWCNTs contained in the soot self-organize into 3D bundles [4,14,16,20], the present ‘all-laser’ process is shown to lead exclusively to a lateral growth of planar (2D) arrays of SWCNTs. Indeed, linescan height profiles (as shown in the inset of Fig. 2b) reveal that only one layer of nanotubes are horizontally arranged on the HOPG surface. More interestingly, it is clearly seen that the 2D arrays are highly oriented making an angle of 120° to one another (see Fig. 2b). Such specific orientations are thought to be due to the underlying graphite hexagonal lattice. These results are not surprising if one recalls the natural tendency of purified SWCNTs to align 120° to one another when dispersed on a HOPG surface [4,20]. Thus, by aligning themselves along the three axes of the basal plane of HOPG, the SWCNTs can form a ‘Y’ branching, where each branch is oriented at 120° to one another, as reported in the case SWCNTs grown from the catalytic decomposition of C_{60} [27]. Indeed, theoretical calculations indicate that the interaction energy of SWCNTs and the underlying HOPG substrate presents a sharp minimum when the two lattice structures are aligned [28]. Such an alignment between the two lattice structures has been recently evidenced by means of atomically resolved STM observations [29]. Thus, our ‘all-laser’ process is shown to offer a relatively easy way for the growth of planar (2D) layers of SWCNTs of which orientations are determined by the underlying HOPG substrate. This sort of epitaxial growth of SWCNTs can be advantageously used not only to investigate their properties in selected orientations but also to integrate them into nanodevices [1,30].

Fig. 3 shows Raman spectra of two different HOPG surfaces, namely (i) the CoNi nanoparticle-decorated HOPG after its subjection to the heat-treatment at 1150°C without any carbon deposition (Fig. 3a) and (ii) the CoNi nanoparticle-decorated HOPG after carbon deposition at 1150°C with 100 laser pulses (Fig. 3b), which is above-shown by STM to lead to the formation of SWCNTs. It is clear from Fig. 3a that without exposing the CoNi decorated HOPG surface to the laser ablated carbon, no carbon nanotube related peaks are detected and the only peak present in the spectrum is the HOPG peak at 1580 cm^{-1} . In contrast, the clear scattering lines appearing in the low- and the high-frequency ranges of Fig. 3b are typical signatures of SWCNTs [31]. Indeed, the Raman lines in the low-frequency region ($180\text{--}250\text{ cm}^{-1}$) are due to the radial

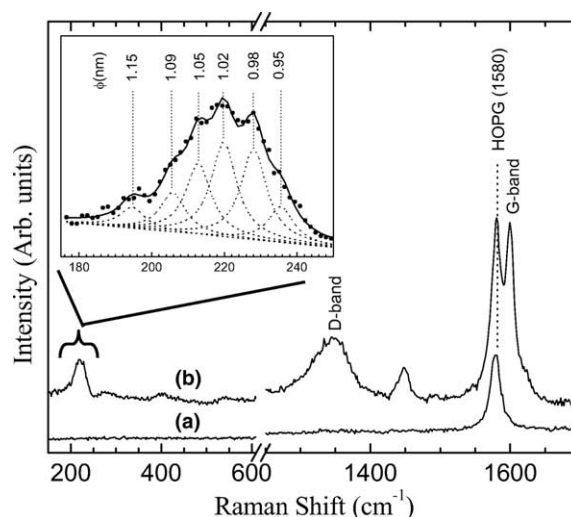


Fig. 3. Raman spectra of (a) a CoNi nanoparticle-decorated HOPG surface heat-treated at 1150°C without the carbon deposition; and (b) a CoNi nanoparticle-decorated HOPG surface after the carbon deposition at 1150°C with 100 laser pulses. The inset shows the details of the low-frequency region of the Raman spectrum. The individual Lorentzian (---) curves used for fitting the experimental RBM band (•) are shown along with the labels showing their corresponding nanotube diameters.

breathing modes (RBM) of single wall nanotubes. The Raman shift (ω_{RBM} , in cm^{-1}) of the RBM mode is related to the SWCNT diameter (d , in nm) by $d = 223.75/\omega_{\text{RBM}}$ [32]. The RBM band was deconvoluted into six Lorentzian components (easily distinguishable on the spectrum by their associated shoulders; see inset of Fig. 3) according to the method described by Pimenta et al. [33]. (All Lorentzians were given the same FWHM of $\sim 8.4\text{ cm}^{-1}$.) The deduced peaks positions are 195, 205, 213, 219, 228, and 236 cm^{-1} which correspond to nanotube diameters (d) of 1.15, 1.09, 1.05, 1.02, 0.98, 0.95 nm, respectively. This result indicates that the SWCNTs grown by the ‘all-laser’ process on HOPG have a narrow diameter distribution. Indeed, by using the six d values weighted by their respective Lorentzian peak area, we end up to an average nanotube diameter of $1.02 \pm 0.05\text{ nm}$, which is in good agreement with the ($1.10 \pm 0.26\text{ nm}$) values deduced from STM analyses. In addition there are two others peaks, namely at 1346 and 1450 cm^{-1} Raman shift positions. While the latter peak has not been observed previously (its origin remains unclear), the former (at 1346 cm^{-1}) is due to the D-band. Its broad shape could be indicative of the presence of some amorphous carbon on HOPG surface.

Finally, we point out that the ‘all-laser’ process we have developed is highly efficient in converting the laser ablated graphite carbon into SWCNTs. Indeed, by decreasing the amount of ablated carbon to only 5 laser ablation bursts (which would correspond to an equivalent carbon coating layer of $\sim 0.2\text{ nm}$ -thick), 2D arrays of aligned SWCNTs similar to those obtained with 100

pulses were grown on the HOPG substrate (Fig. 4a). Their corresponding diameter and average length (taken from 40 nanotubes in various STM images) are of about (0.8 ± 0.2) nm and ~ 40 nm, respectively. These values are somewhat smaller than those of the SWCNTs obtained with 100 laser pulses. Indeed, a more systematic investigation of the effect of the ablated amount of carbon on the SWCNTs characteristics revealed that, while the average diameter of the nanotubes remains almost unchanged (Fig. 4b, left-hand scale), the nanotube mean length is found to increase monotonically with the number of laser pulses (Fig. 4b, right-hand scale). This tube

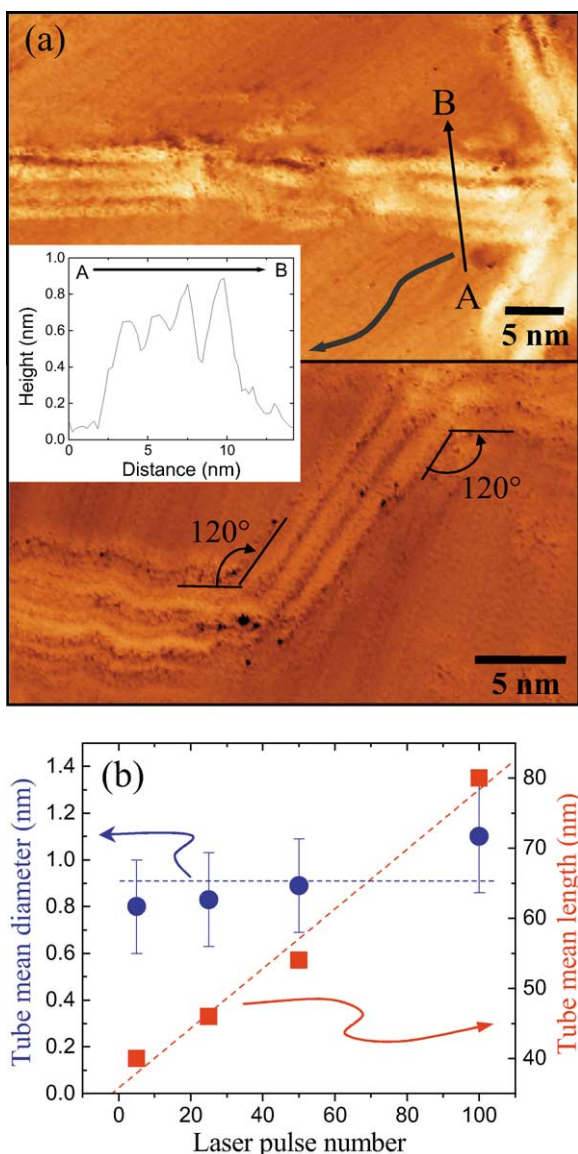


Fig. 4. (a) STM image of SWCNTs grown on CoNi decorated HOPG with only five laser ablation pulses of graphite. (b) The mean diameter and tube length of SWCNTs as a function of the number of laser ablation pulses of graphite. The inset is a linescan height profile of A–B line in the image (a).

length dependence on carbon amount available from the ablation of the graphite target can be interpreted as the result of a significant diffusion of the carbon atoms on the HOPG surface, particularly when one considers the weak energy barriers (~ 0.03 eV/nm) for the sliding motion of SWCNTs on HOPG [23,28,34]. However, a more complete mechanism (taking into account not only the nanoparticle–nanotube relationship but also the non-equilibrium aspect of the laser ablation of graphite) for the growth of our nanotubes is still to be established.

4. Conclusion

In conclusion, we have demonstrated for the first time the growth of highly oriented and exclusively planar arrays of SWCNTs on HOPG substrates by means of an ‘all-laser’ growth process. While these epitaxially grown SWCNTs are found to exhibit a narrow diameter distribution, their mean length can be adjusted at will by controlling the amount of laser ablated graphite. In addition, our ‘all-laser’ process is found to have an unprecedented efficiency for converting graphite carbon into SWCNTs. Indeed, only very few laser shots are sufficient to grow easily observable arrays of SWCNTs onto the CoNi decorated HOPG substrates. Finally, the ability of controlling the orientation of planar arrays of SWCNTs, as shown in the present work, will definitely open new prospects not only for the investigation of their properties in specific directions but also for the achievement of nanodevices.

Acknowledgments

This work was financially supported by the Québec Research Network in Nanoscience and Nanotechnology (NanoQuébec) and the Natural Science and Engineering Research Council (NSERC) of Canada.

References

- [1] A. Cao, X. Zhang, C. Xu, J. Liang, D. Wu, X. Chen, B. Wie, P.M. Ajayan, *Appl. Phys. Lett.* 79 (2001) 1252.
- [2] S.J. Wind, J. Appenzeller, Ph. Avouris, *Phys. Rev. Lett.* 91 (2003) 058301.
- [3] R.H. Baughman, A.A. Zakhidov, W.A. Heer, *Science* 297 (2002) 787.
- [4] H. Yanagi, E. Sawada, A. Manivannan, L.A. Nagahara, *Appl. Phys. Lett.* 78 (2001) 1355.
- [5] V. Derycke, R. Martel, M. Radosavljević, F.M. Ross, Ph. Avouris, *Nano Lett.* 2 (2002) 1043.
- [6] N.R. Franklin, Q. Wang, T.W. Tomblor, A. Javey, M. Shim, H. Dai, *Appl. Phys. Lett.* 81 (2002) 913.
- [7] K.H. Lee, J.M. Cho, W. Sigmund, *Appl. Phys. Lett.* 82 (2003) 448.
- [8] T. Dürkop, S.A. Getty, E. Cobas, M.S. Fuhrer, *Nano Lett.* 4 (2004) 35.

- [9] H. Dai, *Acc. Chem. Res.* 35 (2002) 1035.
- [10] A. Ural, Y. Li, H. Dai, *Appl. Phys. Lett.* 81 (2002) 3464.
- [11] S.D. Scott, S. Arepalli, P. Nikolaev, R.E. Smalley, *Appl. Phys. A* 72 (2001) 573.
- [12] A. Thess, R. Lee, P. Nikolaev, H. Dai, P. Petit, J. Robert, C. Xu, Y.H. Lee, S.G. Kim, A.G. Rinzler, D.T. Colbert, G.E. Scuseria, D. Tománek, J.E. Ficher, R.E. Smalley, *Science* 273 (1996) 483.
- [13] T. Guo, P. Nikolaev, A. Thess, D.T. Colbert, R.E. Smalley, *Chem. Phys. Lett.* 243 (1995) 49.
- [14] N. Braidy, M.A. El Khakani, G.A. Botton, *Chem. Phys. Lett.* 354 (2002) 88.
- [15] M. Yudasaka, Y. Kasuya, F. Kokai, K. Takahashi, M. Takizawa, S. Bandow, S. Iijima, *Appl. Phys. A* 74 (2002) 377.
- [16] N. Braidy, M.A. El Khakani, G.A. Botton, *Carbon* 40 (2002) 2835.
- [17] S. Arepalli, C.D. Scott, P. Nikolaev, R.E. Smalley, *Chem. Phys. Lett.* 320 (2000) 26.
- [18] N. Braidy, M.A. El Khakani, G.A. Botton, *Mat. Res. Symp. Proc.* 703 (2002) 407.
- [19] N. Braidy, M.A. El Khakani, G.A. Botton, *J. Mater. Res.* 17 (2002) 2189.
- [20] J. Liu, A.G. Rinzler, H.J. Dai, J.H. Hafner, R.K. Bradley, P.J. Boul, A. Lu, T. Iverson, K. Shelimov, C.B. Huffman, F. Rodriguez-Macias, Y.S. Shon, T.R. Lee, D.T. Colbert, R.E. Smalley, *Science* 280 (1998) 1253.
- [21] M.A. El Khakani, J.H. Yi, *Nanotechnology* 15 (2004) S534.
- [22] H. Dai, J. Kong, C. Zhou, N. Franklin, T. Tomblor, A. Cassell, S. Fan, M. Chapline, *J. Phys. Chem. B* 103 (1999) 11246.
- [23] H. Hövel, M. Bödecker, B. Grimm, C. Rettig, *J. Appl. Phys.* 92 (2002) 771.
- [24] A. Maiti, C.J. Brabec, J. Bernholc, *Phys. Rev. B* 55 (1997) 6097.
- [25] Q. Jiang, J.C. Li, B.Q. Chi, *Chem. Phys. Lett.* 366 (2002) 551.
- [26] M.A. El Khakani, J.H. Yi, B. Aïssa, *Diam. Relat. Mater.* (to be published).
- [27] P. Nagy, R. Ehlich, L.P. Biro, J. Gyulai, *Appl. Phys. A* 70 (2000) 481.
- [28] A. Buldum, P.L. Jiang, *Phys. Rev. Lett.* 83 (1999) 5050.
- [29] C. Rettig, M. Bödecker, H. Hövel, *J. Phys. D: Appl. Phys.* 36 (2003) 818.
- [30] A. Cassell, N. Franklin, T. Tomblor, E. Chan, J. Han, H. Dai, *J. Am. Chem. Soc.* 121 (1999) 7975.
- [31] A.M. Rao, E. Richter, S. Bandow, B. Chase, P.C. Eklund, K.A. Williams, S. Fang, K.R. Subbaswamy, M. Menon, A. Thess, R.E. Smalley, G. Dresselhaus, M.S. Dresselhaus, *Science* 275 (1997) 187.
- [32] S. Bandow, S. Asaka, Y. Saito, A.M. Rao, L. Grigorian, E. Richter, P.C. Eklund, *Phys. Rev. Lett.* 80 (1998) 3779.
- [33] M.A. Pimenta, A. Marucci, S.D.M. Brown, M.J. Matthews, A.M. Rao, P.C. Eklund, R.E. Smalley, G. Dresselhaus, M.S. Dresselhaus, *J. Mater. Res.* 13 (1998) 2396.
- [34] M.R. Falvo, J. Steele, R.M. Taylor II, R. Superfine, *Phys. Rev. B* 62 (2002) 10665.